

Transformation of electromagnetic waves and sound in tungsten in a magnetic field

A. V. Golik, A. P. Korolyuk, V. A. Fal'ko, and V. I. Khizhnyi

Institute of Radiophysics and Electronics, Ukrainian Academy of Sciences

(Submitted 7 June 1983)

Zh. Eksp. Teor. Fiz. **86**, 616–626 (February 1984)

The transformation of electromagnetic and transverse sound waves in a plane-parallel tungsten plate is studied at 4.2 K in the nonlocal limit, when $ql > 1$ (q is the sound wave vector and l the electron mean free path). The experiments are carried out at frequencies 20–200 MHz in magnetic fields up to 60 kOe. The dependence of the transformation amplitude on the magnetic field intensity is studied for the $q \parallel H \parallel [100]$ geometry. It is shown experimentally that the transformation is due to the simultaneous action of a deformation force and an induction force. By applying linearly polarized exciting electromagnetic waves, we can separate the induction and deformation contributions experimentally. Nonmonotonic dependences of the induction and deformation transformation mechanisms on the magnetic field are observed in the region $qR > 1$ (R is the cyclotron radius of the conduction electron). The effect of rotation of the plane of polarization of the generated acoustic waves is observed and explained. Nonmonotonic dependences of the angle of rotation of the plane of polarization of the generated sound and the ellipticity are observed under the conditions of Doppler-shifted cyclotron resonance (DSCR) and Doppler-phonon resonance (DPR). A method is proposed for determining the doppleron attenuation distance under doppleron-phonon resonance conditions for the direct transformation of electromagnetic waves into sound. The attenuation distance of a G -doppleron is determined experimentally.

INTRODUCTION

The effects of the transformation of electromagnetic and sound waves, due to the interaction of conduction electrons with the electromagnetic wave and the crystal lattice, under conditions of weak spatial inhomogeneity (in the case in which the inequality $ql \ll 1$ is valid, where q is the wave number of the sound and l is the free path length of the conduction electrons) have been studied in many experimental and theoretical works.^{1,2} The experimental investigation of the transformation of waves in an external constant magnetic field in the nonlocal limit ($ql > 1$) is of special interest, since under these conditions the appearance of different electromagnetic and magneto-acoustic resonances are possible, as well as effects of coupling of the characteristic electromagnetic modes of the electron-hole plasma with the sound. At the present time, the following magneto-acoustic effects have been studied in the transformation regime: quantum oscillations in a strong magnetic field,^{3–7} and geometric resonance in copper and silver.⁸ We reported earlier^{9,10} on the observation of Doppler-shifted cyclotron resonance (DSCR) and Doppler-phonon resonances (DPR) in tungsten in the transformation regime.

The present work is devoted to the study of mechanisms of mutual transformation of electromagnetic waves and sound, resonant phenomena, and the effects of polarization of the generated sound in tungsten over a wide range of magnetic fields, in a geometry in which the wave vector of the sound q and the vector of the constant magnetic field H are perpendicular to the surface of the sample.

EXPERIMENTAL METHOD

For the study of the high-frequency transformation of electromagnetic waves and sound, we chose the “in trans-

mission” method of work in which, a tungsten sample¹⁾ an acoustic signal was excited or recorded, and on the other side an electromagnetic signal (Fig. 1). In contrast with our first experiments,^{9,10} special attention was paid here to the prevention of direct penetration of the electromagnetic signal into the surrounding of the sample. With the help of special gaskets, we could lower the level of seepage below the threshold of sensitivity of the detecting circuit, which was equal to 125–130 dB/W. These measures, and also the elimination of loss by complete matching of the piezotransducer and the electromagnetic circuit to coaxial lines, made it possible to carry out amplitude measurements at an applied rf power from the generator to below 30 mW. The measurements were made at frequencies of 20–200 MHz in the cw regime, in a geometry $q \parallel H \parallel [100]$. Practically all the experiments were performed at 4.2 K.

Since the measurements of the dependence of the transformation on the magnetic field were carried out in a cw

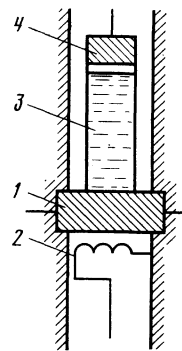


FIG. 1. Experimental scheme: 1—sample, 2—electromagnetic circuit, 3—ultrasonic delay line, 4—acoustic transducer.

regime, the necessity arose of estimating the linear damping of the generated acoustic or electromagnetic wave. At low damping, multiple reflections of the generated wave are possible in the sample, and the resultant signal on the receiving side in this case is the sum of signals from the different passes, which materially complicates the interpretation of the experimental results. For an estimate of the damping of the generated wave after a single pass, we used the method of frequency "rocking." Figure 1 shows the amplitude-frequency characteristics (AFC) of a tungsten sample in the transformation regime.

The shape of the Fabry-Perot resonance line in the transformation regime can be described by analogy with the acoustic method¹¹ by summing the multiple passes of the generated wave. Extraneous losses in the resonator, due to the nonmatching of the acoustic and electromagnetic impedances at the boundaries, were taken into account by the introduction of a reflection coefficient $P_0 = (P_1 P_2)^{1/2}$, where P_1 and P_2 are the reflection coefficients from the different boundaries of the sample. The shape of the resonance line has the form

$$|U| = A (\text{sh}^2 \xi \cos^2 qd + \text{ch}^2 \xi \sin^2 qd)^{-1/2}, \quad (1)$$

where $A = f(U_0, P_0)$, U_0 is the amplitude of the wave incident on the sample, $\xi = \Gamma_0 d + |\ln P_0|$ is the total damping per pass, Γ_0 is the damping, $|\ln P|$ are the "outside" losses, d is the thickness of the sample. Equation (1) is obtained by summation of a geometric progression of the form

$$U = \sum_{n=1}^{\infty} U_0 (1 - P_0)^2 P_0^{2(n-1)} \exp[-(2n-1)(\Gamma_0 d + iqd)].$$

The small change in the phase of the reflections of the wave can be neglected, since it leads to a small change in the resonance frequencies and does not affect in any essential way the quality factor of the resonator, which, at the half-power level, is equal to

$$Q = n\pi/2 \arcsin \text{sh} \xi. \quad (2)$$

The dependence of the quality factor of the resonator on the frequency, Fig. 2a, is connected with the change in the reflection coefficient P_0 . In the region of the center of the AFC ($\omega/2\pi = 55$ MHz), the acoustic impedances of the sample and transducer are matched, and the reflection from the boundaries is minimal. A comparison of the experimentally observed AFC with Eqs. (1) and (2) allows us to make the estimate $P_0 < 0.7$; $\xi \gtrsim 0.6$, where $Q \approx 180-200$, $d = 2$ mm, the sound velocity $v = 2.9 \times 10^5$ cm/s. These results are in excellent agreement with the data obtained from pulse methods. The ratio of the amplitudes of the pulse, with duration of 0.5 μ s and with carrier frequency 55 MHz, after 1 and 3 passes amounted to 4, which yields an estimate of $\xi \approx 0.7-0.8$ for the damping, i.e., in the transformation regime, the linear damping of the wave in the sample at a frequency of 55 MHz is 3 dB/mm. In a magnetic field, the value of the damping ξ at $ql \gg 1$ does not remain constant; however, as experiment has shown, over the entire region of magnetic fields studied, its changes were appreciably below 1 dB/mm. The results of Refs. 12 and 13 allow us to extrapolate the obtained estimates of damping in a linear way, which yields, for the fre-

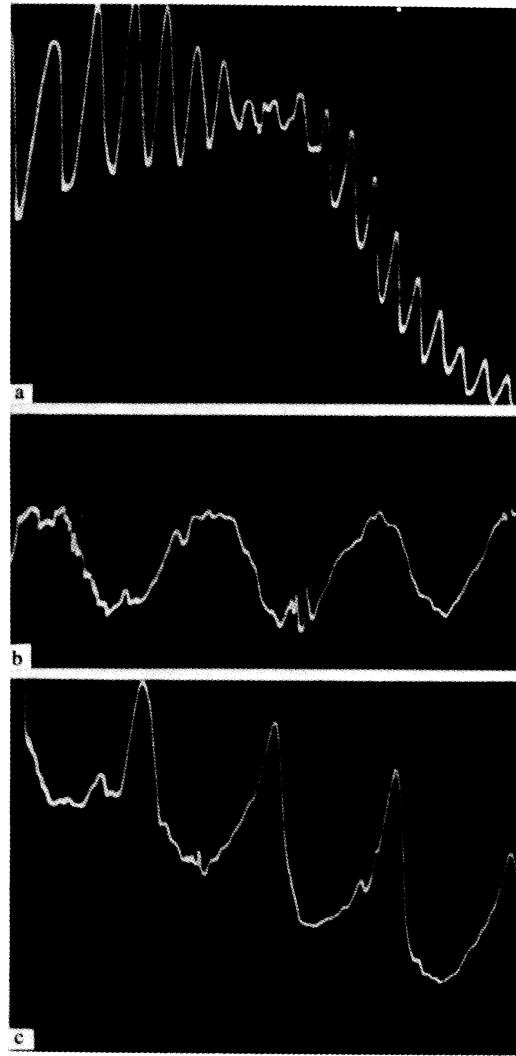


FIG. 2. Amplitude-frequency characteristics of a tungsten sample in the transformation regime: a—sweep range 40–70 MHz, $H = 8$ kOe; b—sweep near the fundamental frequency of the transducer $\omega/2\pi = 55$ MHz, $H = 0$; c—sweep on the "slope" (right wing) of the amplitude-frequency characteristic of the transducer ~ 65 MHz, $H = 30$ kOe. The distance between markers in Figs. 2b and c is equal to 1 MHz.

quency ≈ 150 MHz, an estimate of 9–10 dB/mm. Consequently, in the analysis of the experimental results we can, with sufficient accuracy, neglect the effect of multiple reflections for frequencies greater than 100 MHz. At frequencies below 100 MHz, it is necessary to introduce a correction coefficient in the numerical analysis and interpretation of the experimental results, of the type $\cosh \xi d / \sinh \xi d$, which takes the effects of multiple reflections into consideration.

EXPERIMENTAL RESULTS

All the experimental records are independent of the direction of the transformation at the appropriate sign of \mathbf{H} , i.e., the electromagnetic generation of the sound was identical to the acoustic generation of the electromagnetic wave.

To distinguish the mechanisms of transformation and for investigation of the polarization effects, the field dependences were recorded at different mutual orientations of the plane of polarization of the piezotransducer and the electro-

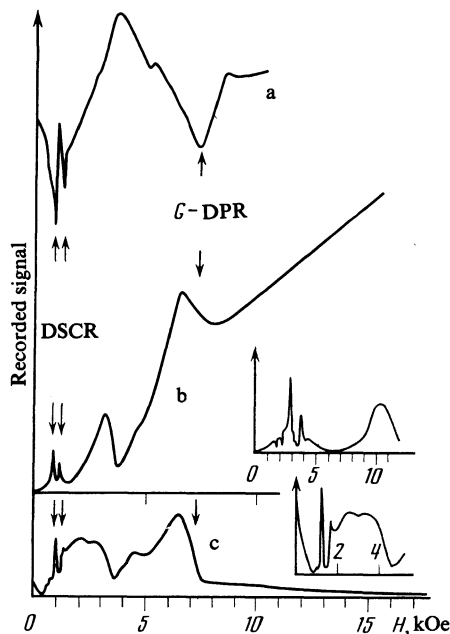


FIG. 3. Amplitude dependences of the recorded signals on the magnetic field: a—0 sound-sound, $\omega/2\pi = 55$ MHz; b—transformation $U_{\perp}(H)$, $\omega/2\pi = 55$ MHz, inset— $\omega/2\pi = 155$ MHz; c—transformation $U_{\parallel}(H)$, $\omega/2\pi = 55$ MHz, inset— $\omega/2\pi = 68.4$ MHz.

magnetic circuit. In Fig. 3b, c are shown the field dependences of the transformation at a frequency of 55 MHz and, for comparison, Fig. 3a shows the sound absorption coefficient, when the polarization axes of the two transducers are parallel. The plot in Fig. 3a is analogous to that obtained earlier in Ref. 14. Figure 3a gives the $U_{\perp}(H)$ and $U_{\parallel}(H)$ dependences when the electric field vector of the wave on the surface of the sample, $E(0)$, and the plane of polarization of the transducer are perpendicular (3b) and parallel (3c). The recordings in the insets of Figs. 3b, c were made at 155 and 68 MHz, respectively, under the same mutual orientations of the transducer and electric field $E(0)$.

At a frequency of 55 MHz and in a range of fields above 10 kOe, a decrease of $U_{\parallel}(H)$ virtually to zero has been observed. At the same time, $U_{\perp}(H)$ increases with increase in H according to a linear law. Such a dependence of $U_{\perp}(H)$ is observed up to 60 kOe at a frequency of 150 MHz at 4.2 K. In this region of fields, $U_{\parallel}(H) \ll U_{\perp}(H)$, i.e., the polarization of the generated sound is perpendicular to $E(0)$. At a frequency $\omega/2\pi = 55$ MHz, in fields below 10 kOe, resonance features are observed in the dependences of $U_{\perp}(H)$ and $U_{\parallel}(H)$, as well as in the sound absorption. An anomaly at $H \approx 8$ kOe for the components $U_{\parallel}(H)$ and $U_{\perp}(H)$ is the appearance of DPR in the transformation regime. A second anomaly in the field $H \leq 3$ kOe in $U_{\parallel}(H)$ appears in the form of a step, and in $U_{\perp}(H)$ in the form of a resonance, similar in form with the DPR at $H = 8$ kOe. In the sound absorption (Fig. 3a), this singularity is practically unseen. At $H \leq 1$ kOe, DSCR appear in the transformation. At limitingly small magnetic fields and at $H = 0$, a transformation is observed only for $U_{\parallel}(H)$ and the vector of the polarization of the generated sound at $H = 0$ is parallel to $E(0)$.

In all the experiments with different angles φ of the mutual orientation of the planes of polarization of the elec-

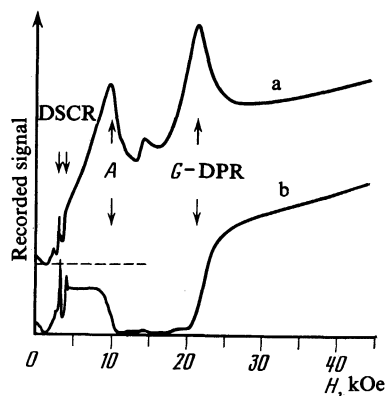


FIG. 4. Amplitude dependence of the recorded transformation signal on the inversion of the magnetic field, $\omega/2\pi = 155$ MHz, the angle between the axis of polarization of the transducer and the vector $E(0)$, $\varphi = (25 \pm 2)^\circ$; a—recording at $+H$, b—recording at $-H$.

tromagnetic circuit and the piezotransducer, recordings were made in the regime of reversal of the magnetic field, i.e., with the substitution of $-H$ for $+H$. The method of magnetic field reversal was suggested for magnetoacoustic measurements in Ref. 15. The field dependences $U_{\perp}(H)$ and $U_{\parallel}(H)$ of Figs. 3b, c ($\varphi = 90^\circ$ and 0°) were not very sensitive to reversal of the magnetic field if the deviation of the angle φ from 0° and 90° did not exceed a few degrees. The most significant difference in the amplitudes of the transformation in the magnetic field corresponding to DFR were at $\varphi = (25 \pm 2)^\circ$. This record at a frequency of $\varphi/2\pi = 155$ MHz is shown in Fig. 4. For the field $-H$ an interval of 10 kOe was observed in the field dependence in which the signal of the transformation was virtually absent. The edges of this region—the “steps”—correspond to resonance anomalies in the direction of the magnetic field $+H$.

DISCUSSION OF THE EXPERIMENTAL RESULTS

First of all, we note that when the vectors q and H are not strictly parallel, the appearance of effects in the field dependences $U(H)$ are possible (the type of DSCR or its harmonics, lifting of the degeneracy in the two acoustic modes) that are due to the lowering of the symmetry of the experiment. However, if the departures from parallelism do not exceed $1.5-2^\circ$, these effects cannot be observed with sufficient accuracy.

The transformation of an electromagnetic wave into an acoustic one, under the conditions in which q and H are perpendicular to the surface of the sample, has been considered theoretically for a semi-infinite metal with a single type of quasiparticle and with a spherical Fermi surface,^{16,17} and for a metal plate with a complicated Fermi surface for electrons and holes.¹⁸ For the interpretation of the experimental results, we set down some results from Ref. 18. Subject to the inequalities that are satisfied under the conditions of the given experiment,

$$L_s > d > l, L_D, \delta, \quad (3)$$

(where L_s is the damping distance of the sound, L_D is the damping distance of the characteristic electromagnetic

mode, δ is the skin depth), the amplitude of the circularly polarized sound that is generated has the form

$$U_s = \frac{\alpha_s q_s}{\rho \omega^2} \exp(iq_s d) \frac{-2E'(0)}{q_s^2 - i(4\pi\omega/c^2) \sigma_s(q_s, H)} \quad (4)$$

$$\times \left\{ \frac{H}{c} \operatorname{sgn} \sigma_s(q_s, H) + q_s \eta_s(q_s, H) \right\}.$$

Here the index s denotes the polarizations $+$ or $-$, $U_{\pm} = U_x \pm iU_y$; the system of coordinates is chosen in the following way: the Z axis is parallel to the vectors \mathbf{q} and \mathbf{H} , the X axis is directed along the vector of the electric field of the electromagnetic wave in a vacuum, $\mathbf{E}(0)$; further, $E'(0) = dE(0)/dZ$, q_s is the wave vector of the sound with account of dispersion of the velocity and damping in the sample, ρ is the density of the metal, α_s describes the effect of multiple reflection of the sound from the boundaries. In what follows, the effect of multiple reflection of the sound will not be taken into account, and we shall set $\alpha_s = 1$. In addition,

$$\sigma_s = \sigma_{sx} + i \operatorname{sgn} s \sigma_{yx}, \quad \eta_s = \eta_{sx} + i \operatorname{sgn} s \eta_{yx},$$

$$\sigma_{\alpha\beta} = \sum_n^{(n)} \sigma_{\alpha\beta}^{(n)}, \quad \eta_{\alpha\beta} = \sum_n^{(n)} \eta_{\alpha\beta}^{(n)},$$

where $\sigma_{\alpha\beta}^{(n)}$, $\eta_{\alpha\beta}^{(n)}$ are the tensors of the electric and "deformation" conductivities for an n group of electrons.¹⁸

The first term in (4) describes the induction mechanism of interaction of the conduction electrons with the electromagnetic wave and the crystal lattice, and the second the deformation interaction. These mechanisms lead to different dependences of the sound amplitude U_s on H . Thus, in the non-local limit, in the region of H for which the following inequality is valid,

$$|q_s^2| \ll |i(4\pi\omega/c^2) \sigma_s(q_s, H)| \quad (5)$$

the induction mechanism gives a linear dependence of U_s on H while the deformation mechanism can be the reason for the complicated nonmonotonic dependence on H described by the function η_s/σ_s . For tungsten, the condition (5) is satisfied at not too high frequencies, $\omega \ll 10^{10} \text{ s}^{-1}$, in the range of H that excludes strong magnetic fields (greater than 30 kOe) and the region of resonances of phonons with the weakly damped wave, in which

$$q_s^2 \approx |i(4\pi\omega/c^2) \sigma_s(H)|.$$

Resonance effects were considered in Ref. 18 in the transformation regime, which were due only to the presence of a cross section on the Fermi surface with extremal density of states of the electrons (DSCR), or to a binding of the phonons with the weakly attenuating mode of the plasma of the metal—dopplersons (DPR). The resonances $U_s(H)$ of the first type are connected with the resonance singularities of the functions $\sigma_s(H)$ and $\eta_s(H)$. Upon satisfaction of the inequality (5), they appear only in the deformation term for $U_s(H)$. Resonances of the second type arise when the denominator in (4) becomes resonant, i.e.,

$$\operatorname{Im} \sigma_s(H) < 0, \quad |\operatorname{Im} \sigma_s(H)| > |\operatorname{Re} \sigma_s(H)|, \quad (6)$$

which is the condition for the existence of the weakly attenuated wave. Here both mechanisms, induction and the deformation, can make contributions to $U_s(H)$ of the same order.

As $H \rightarrow 0$, the component U_{\parallel} becomes equal to a constant whose value depends on the parameter ql , while U_{\perp} tends to zero in proportional to H . Upon increase in H the component $U_{\parallel}(H)$ becomes smaller, while $U_{\perp}(H)$ increases. In a sufficiently strong field, when

$$qR(H) < 1, \quad (7)$$

for all the electron groups (R is the cyclotron radius), U_{\parallel} is negligibly small in comparison with U_{\perp} . In the region (5), the generation of U_{\parallel} is entirely due to the deformation mechanism. In the component U_{\perp} , in a compensated metal, the induction and the deformation mechanisms make a contribution of the same order in all regions of H (5). In strong magnetic fields, for which the inequalities (5) and (7) are satisfied simultaneously, U_{\perp} is directly proportional to H . The resonant growth of the amplitude, due to DSCR and DPR, is present in both U_{\perp} and U_{\parallel} and rises above a background that changes monotonically with the magnetic field.

Linearly polarized sound was recorded in the experiments, with components

$$U_x \equiv U_{\parallel} = (U_+ + U_-)/2, \quad U_y \equiv U_{\perp} = (U_+ - U_-)/2i.$$

It follows from (4) and from the symmetry of the experiment that upon inversion of the magnetic field,

$$U_{\parallel}(H) = U_{\parallel}(-H), \quad U_{\perp}(H) = -U_{\perp}(-H), \quad (8)$$

while the absolute value of the vector

$$|U(H)| = |U(-H)|. \quad (9)$$

The functions $\sigma_s(H)$, $\eta_s(H)$ and $q_s(H)$ are essentially different for the polarizations $+$ and $-$ only in the regions of resonances (DSCR, DPR). This leads to the result that in the regions of H close to the resonances, the generated sound should be elliptically polarized in the general case, the major axis of the ellipse being turned relative to the axes of the coordinates. In fields in which there are no resonances, the sound is linearly polarized and the direction of the polarization vector depends on the value of H . The angle $\theta(H)$ between the sound polarization vector and the Y axis is determined by the ratio $U_{\parallel}(H)/U_{\perp}(H)$. It was shown above that for frequencies above 100 MHz, under the condition of our experiments, it suffices to take into account only one pass of the generated wave in the sample. Let the angle of rotation of the plane of polarization of the generated wave in the field $+\mathbf{H}$ be θ ; in the case of reversal from $+\mathbf{H}$ to $-\mathbf{H}$, the plane of polarization of the generated sound is rotated symmetrically relative to X , as is shown in Fig. 5. The projections of the amplitudes U^+ and U^- of the transformed waves in the fields $+\mathbf{H}$ and $-\mathbf{H}$ on the axis of the transducer are equal to

$$U^{\pm} = U(H) |\cos(\varphi \mp \theta)|, \quad (10)$$

where $U(H) \equiv |U(H)|$, and φ is the angle between $\mathbf{E}(0)$ and the transducer axis. It follows from (10) that

$$\operatorname{tg} \theta(H) = [(U^+ - U^-)/(U^+ + U^-)] \operatorname{ctg} \varphi, \quad (11)$$

$$U(H) = 1/2(U^+ + U^-) \begin{cases} (\cos \varphi \cos \theta)^{-1}, \\ (\cos \varphi \sin \theta)^{-1}. \end{cases}$$

The upper sign in (10) and the upper line in (11) are taken at $|\theta| \leq \pi/2 - \varphi$, while the lower ones are taken at $\pi/2 - \varphi < \theta$

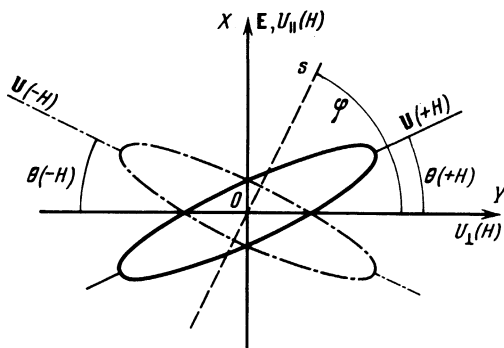


FIG. 5. Polarization of the generated sound $U(H)$ in DPR upon inversion of the magnetic field; s —direction of polarization of the detecting transducer, φ — 0 angle between the axis of polarization of the transducer and the vector $E(0)$, while $\theta(H)$ is the angle of inclination of the major axis of the polarization ellipse.

$< \pi/2 + \varphi$. We note that (10) is valid only for amplitude measurements of small ellipticity, in the absence of a “leakage” signal. The amplitude $U(H)$ is determined with accuracy to an arbitrary factor. Figure 6 shows the $\theta(H)$ and $U(H)$ dependences calculated from (11) for the experimental recording in Fig. 4, and sample thickness $d = 2$ mm. In magnetic fields $H \approx 40$ – 50 kOe, the plane of polarization of the generated sound is almost parallel to Y . Generation in this region of H is due to the induction mechanism, $U_{\perp}(H) \gg U_{\parallel}(H)$ and $\text{tg } \theta \lesssim 5 \times 10^{-2}$. In fields $H \approx 20$ kOe, a jump in the angle of rotation to 22° takes place, which is connected with the DPR. The given DPR in tungsten is due to the nonlocal contribution to the electron conduction from the region of the turning point G of the “knob of the jack” of the Fermi surface of tungsten. In magnetoacoustic measurements, the G -DPR was first identified in Refs. 14 and 19. The corresponding component of generated sound in the field H , equal to the field G -DPR, according to (4) is

$$U_{-} = T_{-} \epsilon_{-}(q_{-}, H) \exp(iq_{-}d),$$

where T_{-} is the nonresonant coefficient of the transformation. The amplitude U_{-} undergoes resonance, and the Fourier component of the electromagnetic field $\epsilon_{-}(q_{-}, H)$ has a resonance maximum at $q \approx k$ (k is the wave vector of the

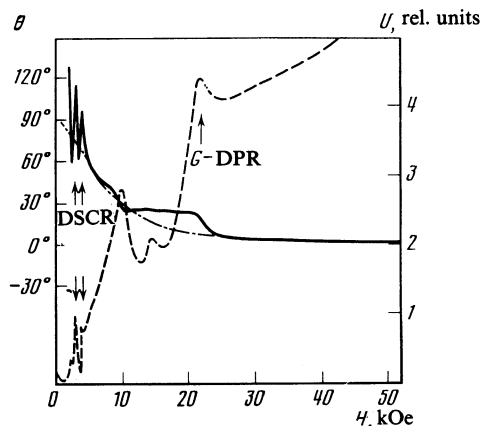


FIG. 6. Dependences of the amplitude $|U(H)|$ (dashed curve) calculated from Fig. 4 and the angle of inclination of the plane of polarization $\theta(H)$ (solid and dot-dash curves).

doppleron), while $\exp(-\text{Im } q_{-}d)$ is the resonance minimum. If the damping distance, the plate thickness and the sound attenuation are such that at the resonance $\epsilon_{-}(q_{-} = k) > \exp(-\text{Im } q_{-}d)$, a resonance maximum is observed in the field dependence $|U(H)|$ and a singularity $\Delta\theta(H) \propto (\text{Re } q_{-} - \text{Re } q_{+})$, is observed in the field dependence $\theta(H)$ and corresponds to the difference in the dispersions of the resonance and nonresonance circular polarizations of the generated mode. In the regime of direct transformation, the angle of rotation of the plane of polarization $\theta(H)$ is due also to the polarization of the background, which is connected with the ratio of $U_{\parallel}(H)$ to $U_{\perp}(H)$.

The ellipticity of the polarization of the generated wave depends essentially on the distribution of the electromagnetic field in the metal, and the study of it in the methodology of the given experiment allows us to give an upper estimate to the damping distance of the dopplerons. The fact that upon reversal of the field H the recorded signal in the vicinity of the DPR was different from zero at any mutual orientation of the axes of polarization of the circuit and the transducer indicates the presence of ellipticity in the transformation regime. The vanishing of the signal in one of the directions of H should indicate that the polarization of the recorded signal is linear and strictly perpendicular to the axis of polarization of the detecting element. This situation is shown in Fig. 4 in fields $10 < H < 20$ kOe. Such a value of the angle $\pi/2 - \varphi \approx (25 \pm 2)^\circ$ corresponds to the minimum value of the signal at $H = H_{\text{DPR}}$ for the direction $-H$. The amplitude of this signal U^{-} is equal, with sufficient accuracy, to the absolute value of the minor axis of the polarization ellipse. The amplitude of the signal U^{+} (in the same experiment) in the field $+H$ is the projection of the major axis r_1 of the polarization ellipse on the axis of the detecting element. It is not difficult to show that $r_1 = U^{+}/\cos 40^\circ$.

For calculation of the damping distance of the doppleron, we rewrite Eq. (4) in the form

$$U_{\pm} = T_{\pm} F_{\pm} \exp(iq_{\pm}d), \quad (12)$$

where T_{\pm} is given by Eq. (4) (the factor in the curly brackets)

$$F_{\pm} = E_{\pm} [q^2 - i4\pi\omega\sigma_{\pm}(q)/c^2]^{-1}.$$

We therefore have $|T_{+}| = |T_{-}|$ with accuracy to within terms of order ν/Ω (Ω is the cyclotron frequency). In the latter formula, E_{\pm} is a constant.

We now calculate the difference in the total attenuations d for the polarizations U_{-} and U_{+} , taking it into account that the doppleron exists in the polarization $-$. In DPR,

$$(k_1 + ik_2)^2 = i4\pi\omega\sigma_{-}(k_D)/c^2, \quad (13)$$

$$|F_{\pm}| = E \{ [q^2 \pm (k_1^2 - k_2^2)]^2 + (2k_1k_2)^2 \}^{-1/2},$$

where $k_D = k_1 + ik_2$ is the wave vector of the doppleron, and E is a constant.

a) For a weakly attenuated doppleron ($k_1 \gg k_2$), we get from (13):

$$|F_{-}| = E(2k_1k_2)^{-1}, \quad |F_{+}| = E(2k_1^2)^{-1}, \quad (14)$$

and

$$\ln(k_1/k_2) = \alpha d + \Delta\Gamma d, \quad q^2 = k_1^2, \quad (15)$$

where $q = \omega/v_s$, $\Delta\Gamma = \Gamma_2^- - \Gamma_2^+$ ($\Gamma_2^- > \Gamma_2^+$; $\alpha d > 0$), and Γ_1^\pm and Γ_2^\pm are the real and imaginary parts, respectively, of the renormalized wave vectors. The value of the difference of the total attenuations αd is determined by the ellipticity r_2/r_1 :

$$\alpha d = \ln \frac{[(r_2/r_1)^2 + 1] \pm 2(r_2/r_1)}{[1 - (r_2/r_1)^2]} \quad (16)$$

b) If the attenuation of the doppleron is not small ($k_1 > k_2$), we have

$$|F_-| = E(2k_1k_2)^{-1}, \quad |F_+| = E[4(k_1^2 - k_2^2)^2 + 4(k_1k_2)^2]^{-1/2} \quad (17)$$

and

$$1/2 \ln [(k_1^2 - k_2^2)^2 / (k_1k_2)^2 + 1] = \alpha d + \Delta\Gamma d.$$

The damping of the doppleron in this case is determined by the expression

$$k_2^2 = q \{ -1/2 + [1/4 + 1/(z-1)]^{-1/2} \}, \quad (18)$$

$$z = [(k_1^2 - k_2^2)^2 / (k_1k_2)^2 + 1], \quad k_1^2 = q^2 + k_2^2. \quad (19)$$

Thus, by measuring the ratio of the semiaxes of the ellipse

$$r_2/r_1 = U^-(-H) / [U^+(+H) \cos^{-1}(\pi/2 - 2\varphi)]$$

under the conditions of inversion of the magnetic field in the case of known φ , as well as the sound absorption $\Delta\Gamma d$ in this same sample under the same conditions, it becomes possible to estimate the damping distance of the dopplerons. This same method can be applied also for estimates of the damping distances of helicons. For the experiments that have been performed, under conditions of "weak coupling," when the mutual repulsion of the branches of the doppleron and the sound spectra is small ($k_1 > k_2$), the parameters measured under the conditions of magnetic field reversal are equal: $\alpha d = 0.2$; $\Delta\Gamma d \approx 0.1$; $r_2/r_1 \approx 0.1$; $\omega/2\pi \approx 155$ MHz; $H = 20$ kOe, and the damping distance of the doppleron is $L_D = 2\pi/k_2 = 1.3\lambda_s$, where λ_s is the sound wavelength. We note that the damping distance obtained for the G -doppleron is much smaller than the mean free path of electrons in tungsten.

The relatively large damping of the G -doppleron at a frequency of 155 MHz leads to a decrease in the DPR in a magnetic field from the position $\lambda_D = \lambda_s$. Actually, the wavelength of the doppleron in DPR is, according to (19),

$$\lambda_D = 2\pi [(2\pi/\lambda_s)^2 + k_2^2]^{-1/2},$$

i.e., $\lambda_D = 0.8\lambda_s$ at $L_D = 1.3\lambda_s$, $H = 20$ kOe, $\omega/2\pi = 155$ MHz. Thus, experiments on the direct transformation of electromagnetic and acoustic waves allow us to determine the dependences of the damping distances of helical electromagnetic waves in metals and semiconductors on various parameters.

In the range of magnetic fields 10–20 kOe, there are flat stretches in the dependence of $\theta(H)$, where $\theta(H) \approx (22-23)^\circ$. The apparent absence of transformation signal in Fig. 4 is due to the fact that the plane of polarization of the recorded wave in a field \mathbf{H} is perpendicular to the axis of polarization of the detector because of the identical change of U_\perp and U_\parallel in the magnetic field.

In a magnetic field $H \approx 10$ kOe, there is a resonance surge in $U(H)$ and a singularity in $\theta(H)$, Fig. 6. The spectrum

of this resonance in $U_\perp(H)$, measured by us in the range of frequencies $\omega/2\pi \approx 20-200$ MHz, corresponded in the coordinates ($q\omega^{-1/3}$; $H\omega^{-1/3}$) to the straight line for A -DPR, with

$$\frac{1}{2\pi} \left(\frac{\partial S}{\partial P_H} \right)_{ext} = 0.5 \text{ \AA}^{-1}$$

(S is the cross section of the Fermi surface in the plane $P_H = \text{const}$). The shape of the A -DPR line in the transformation regime (Fig. 4) differs essentially from its appearance in magneto-acoustic measurements. In the sound absorption coefficient at frequencies up to 200 MHz, the A group on the hole octahedron has a weak absorption peak A -DPR and a step of the "absorption edge" type corresponding to A -DSCR.²⁰ In the transformation, the absence of a surge for $U_\parallel(H)$ can be due to the effect of rotation of the plane of polarization of the generated sound: in the region of A -resonance, as is seen in the $\theta(H)$ dependence, the presence of a jump in the angle $\theta(H)$, corresponding to the range $40-20^\circ$, leads to a decrease in the projection of the amplitude $U(H)$ on the direction X , and an increase in the projection on the Y axis. The relative change in the amplitude at A resonance, which is due to rotation of the plane of polarization is $\Delta U_\parallel / U_\parallel \approx 0.4$, $\Delta U_\perp / U_\perp \approx -0.2$ in accord with Fig. 4. Thus, the "apparent" amplitude in A resonance is the true value for $U_\perp \approx 1.2$ and for $U_\parallel \approx 0.6$. The given estimates are qualitative and require further analysis with the inclusion of specific models of the energy spectrum of the quasiparticles.

In weak magnetic fields $H < 5$ kOe, where $\theta \rightarrow \pi/2$, there is a series of rotations of the plane of polarization of the generated sound in the dependence $\theta(H)$ under DSCR conditions. Such dependences of $\theta(H)$ lead to the result that at $\theta(H) = \pi/2$, the projection of $U(H)$ on the Y axis is equal to zero and singularities of the "antiresonance" type should be observed in the dependence of $U_\perp(H)$ in this range of DSCR. Obviously, the dips in the $U_\perp(H)$ plot (Fig. 3b—insert) are due to just this effect.

The monotonic $\theta(H)$ dependence at a frequency of 155 MHz over the entire range of magnetic fields is well described by the function $\theta(H) = \arctan(\alpha H^{-n})$ at $n = 1.7$. That is, the monotonic variation of the field dependences in large magnetic fields is well approximated by the functions $U_\perp(H) = \alpha_1 H$ and $U_\parallel(H) = \alpha_2 H^{-0.7}$, in agreement with the derivations of Ref. 18.

A satisfactory agreement of theory¹⁸ and experiment exists also in the region of fields in which $qR \gtrsim 1$. Naturally, it is impossible to expect quantitative agreement since effects appear here that are connected with the complicated Fermi surface of tungsten: DPR and DSCR, superposed on the monotonic background of the transformation. Nevertheless, the fact of the essential decrease in the transformation signal for $U_\parallel(H)$ at extremely small magnetic fields (Fig. 3c—insert), when $qR \gg 1$ and for all groups, is not explained by the theory, which, for this region of fields, gives $U_\parallel(H) \text{ const}$.

The authors thank É. A. Kaner for discussion of the present research and S. V. Plyushchev for preparation of single crystals of tungsten of high purity.

¹⁸The initial single crystal of tungsten was grown in the Institute of Solid State Physics, Academy of Sciences USSR.

- ¹J. Mertshing, Phys. St. Sol. **37**, 465 (1970).
- ²E. R. Dobbs, Physical Acoustics, Principles and Methods, Vol. X, 1973, p. 127.
- ³E. R. Dobbs, R. L. Thomas, and D. Hsu, Phys. Lett. **30A**, 338 (1969).
- ⁴E. R. Dobbs, J. Phys. Chem. Sol. **31**, 1657 (1970).
- ⁵R. L. Thomas and D. Hsu, J. Phys. Chem. Sol. Suppl. **132**, 97 (1971).
- ⁶V. F. Gantmakher and V. T. Dolgoplov, Zh. Eksp. Teor. Fiz. **57**, 132 (1969) [Sov. Phys. JETP **30**, 79 (1970)].
- ⁷Yu. P. Gaidukov and A. P. Perov, Pis'ma Zh. Eksp. Teor. Fiz. **8**, 666 (1968) [JETP Lett. **8**, 412 (1968)].
- ⁸M. R. Gaertner and B. W. Maxfield, Phys. Rev. Lett. **29**, 654 (1972).
- ⁹A. V. Golik, A. P. Korolyuk, and V. I. Khizhnyi, Fiz. Nizhn. Temp. **8**, 994 (1982) [Sov. J. Low Temp. Phys. **8**, 502 (1972)].
- ¹⁰A. V. Golik, A. P. Korolyuk, and V. I. Khizhnyi, Sol. St. Comm. **44**, 173 (1982).
- ¹¹V. I. Beletskii, A. P. Korolyuk, and M. A. Obolenskiĭ, PTE, No. 5, 233 (1971).
- ¹²C. K. Jones and J. A. Rayne, Phys. Lett. **13**, 282 (1964).
- ¹³K. B. Vlasov, A. B. Rinkevich, and A. M. Burkhanov, Fiz. Metal. Metall. **53**, 295 (1982).
- ¹⁴T. F. Butenko, V. T. Vitchinkin, A. A. Galkin *et al.*, Zh. Eksp. Teor. Fiz. **78**, 1811 (1980) [Sov. Phys. JETP **51**, 909 (1980)].
- ¹⁵J. R. Boyd and J. D. Gavenda, Phys. Rev. **152**, 645 (1966).
- ¹⁶E. A. Kaner and V. L. Fal'ko, Zh. Eksp. Teor. Fiz. **64**, 1016 (1973) [Sov. Phys. JETP **37**, 516 (1973)].
- ¹⁷G. Reyder, E. Kartheuser, L. R. Ram Mohan, and S. Rodriguez, Phys. Rev. **15B**, 7141 (1982).
- ¹⁸V. L. Fal'ko, Zh. Eksp. Teor. Fiz. **85**, 300 (1983) [Sov. Phys. JETP **58**, 175 (1983)].
- ¹⁹A. A. Galkin, L. T. Tsymbal, T. F. Butenko, A. N. Cherkasov, and A. M. Grishin, Phys. Lett. **67A**, 207 (1978).
- ²⁰A. A. Galkin, L. T. Tsymbal, and A. N. Cherkasov, Pis'ma Zh. Eksp. Teor. Fiz. **33**, 3 (1981) [JETP Lett. **33**, 1 (1981)].

Translated by R. T. Beyer